Journal of Inorganic Biochemistry xxx (2013) xxx–xxx

Contents lists available at SciVerse ScienceDirect

Journal of Inorganic Biochemistry

journal homepage: www.elsevier.com/locate/jinorgbio

Structural insights on the molecular recognition patterns between N^6-substituted adenines and N-(aryl-methyl)iminodiacetate copper(II) chelates ☆

Alicia Domínguez-Martín [a,*], Ángel García-Raso [b], Catalina Cabot [c], Duane Choquesillo-Lazarte [d], Inmaculada Pérez-Toro [a], Antonio Matilla-Hernández [a], Alfonso Castiñeiras [e], Juan Niclós-Gutiérrez [a]

[a] Department of Inorganic Chemistry, Faculty of Pharmacy, Campus Cartuja, University of Granada, E-18071 Granada, Spain
[b] Department of Chemistry, Group of Bioinorganic and Bioorganic Chemistry, University of Illes Balears, E-07122 Palma, Spain
[c] Department of Biology, Group of Bioinorganic and Bioorganic Chemistry, University of Illes Balears, E-07122 Palma, Spain
[d] Laboratorio de Estudios Cristalográficos, IACT, CSIC-Universidad de Granada, Av. de las Palmeras 4, E-18100 Armilla, Granada, Spain
[e] Department of Inorganic Chemistry, Faculty of Pharmacy, University of Santiago de Compostela, E-15782 Santiago de Compostela, Spain

ARTICLE INFO

Article history:
Received 2 December 2012
Received in revised form 7 February 2013
Accepted 8 February 2013
Available online xxxx

Keywords:
N6-substituted adenines
Mixed-ligand copper(II) complexes
Molecular recognition
Interligand interaction
Iminodiacetate
Cytokinin activity bioassays

ABSTRACT

For a better understanding of the metal binding pattern of N^6-substituted adenines, six novel ternary Cu(II) complexes have been structurally characterized by single crystal X-ray diffraction: $[Cu(NBzIDA)(HCy5ade)(H_2O)]\cdot H_2O$ (**1**), $[Cu(NBzIDA)(HCy6ade)(H_2O)]\cdot H_2O$ (**2**), $[Cu(FurIDA)(HCy6ade)(H_2O)]\cdot H_2O$ (**3**), $[Cu(MEBIDA)(HBAP)(H_2O)]\cdot H_2O$ (**4**), $[Cu(FurIDA)(HBAP)]_n$ (**5**) and $\{[Cu(NBzIDA)(HdimAP)]\cdot H_2O\}_n$ (**6**). In these compounds NBzIDA, FurIDA and MEBIDA are N-substituted iminodiacetates with a non-coordinating aryl-methyl pendant arm (benzyl in NBzIDA, p-tolyl in MEBIDA and furfuryl in FurIDA) whereas HBAP, HCy5ade, HCy6ade and HdimAP are N^6-substituted adenine derivatives with a N-benzyl, N-cyclopentyl, N-cyclohexyl or two N-methyl groups, respectively. Regardless of the molecular (**1**–**4**) or polymeric (**5**–**6**) nature of the studied compounds, the Cu(II) centre exhibits a type 4 + 1 coordination where the tridentate IDA-like chelators adopt a *mer*-conformation. In **1**–**5** the N^6-R-adenines use their most stable tautomer H(N9)adenine-like, and molecular recognition consists of the cooperation of the Cu – N3(purine) bond and the intra-molecular interligand N9 – H · · · O(coordinated carboxy) interaction. In contrast, N^6,N^6-dimethyl-adenine shows the rare tautomer H(N3)dimAP in **6**, so that the molecular recognition with the Cu(NBzIDA) chelate consist of the Cu – N9 bond and the N3 – H · · · O intra-molecular interligand interaction. Contrastingly to the cytokinin activity found in the free ligands HBAP (natural cytokinin), HCy5ade and HCy6ade, the corresponding Cu(II) ternary complexes did not show any activity.

1. Introduction

After the discovery of the antitumoral pro-drug Cisplatin by B. Rosenberg in the 1960s [1], a large number of research groups have been focused on the field of metal–nucleic acid complexes. Indeed, during the last decades, much effort has been made to rationalize the metal binding modes of nucleobases, nucleosides and nucleotides, and/or their derivatives, with transition metal ions [2–6]. This is based on the idea that the in-depth study of the chemistry of this kind of ligands, including non-covalent interactions, will allow us to better understand the biochemical processes within biological systems and therefore to build up novel bio-mimetic systems with therapeutic interest. In particular, our research group has been devoted to the study of the metal binding patterns of adenine, which has proved to behave as a fairly versatile ligand in its neutral form, where proton tautomerism phenomena enhance the possibilities of diverse molecular recognition patterns, but also in its different anionic and cationic forms [5]. For instance, neutral adenine (Hade) is able to recognize several Cu(II)-iminodiacetate-like chelates in different ways. Thus, Cu(N-alkyl-iminodiacetate) chelates bind Hade by the Cu – N7 bond reinforced by a N6 – H · · · O interaction while the Cu(N-benzyl-iminodiacetate) [Cu(NBzIDA)] and Cu(N-p-methylbenzyl-iminodiacetate) [Cu(MEBIDA)] chelates bind adenine via N3 and such coordination bond is in cooperation with the N9 – H · · · O interaction [7]. Notably, the reaction of Cu(NBzIDA) chelate and the complementary base-pair adenine:thymine yields the binuclear compound $[Cu_2(NBzIDA)_2(H_2O)_2(\mu_2\text{-N7,N9-Hade})]\cdot 3H_2O$. In this latter compound, adenine exhibits the rare tautomer H(N3)ade and the Cu – N7 and Cu – N9 bonds are assisted by the N6 – H · · · O and N3 – H · · · O interactions, respectively [8].

For a long time, the research on N-substituted adenines has been a topic of great interest. In this context, a huge number of structures have been reported for N9-blocked adenine-like ligands because of their similarities with the building blocks of nucleic acids [9–11]. Likewise, the study of N1, N3 and N7-(heterocyclic) substituted adenines has also been addressed [12–14]. However, the chemistry of N^6-substituted

☆ Dedicated to Prof. Ivano Bertini, outstanding scientist, for his relevant contribution to the Bioinorganic Chemistry field.

* Corresponding author. Tel.: +34 958243853; fax: +34 958246219.
E-mail address: adominguez@ugr.es (A. Domínguez-Martín).

0162-0134/$ – see front matter © 2013 Elsevier Inc. All rights reserved.
http://dx.doi.org/10.1016/j.jinorgbio.2013.02.002

adenines was rather unexplored until the discovery of their presence in plant physiology [15] where these compounds are included in the family of plant hormones called cytokinins [16]. The main difference between these N^6- and the rest of N-heterocyclic substituted adenines is that substitutions in the exocyclic amino group still allow proton tautomerism in the adenine moiety, and this fact may contribute to a higher versatile coordination. In this context, an increasing number of papers has been published in the past years related either to their physiological role in plants [17,18] or to their metal binding properties [19–21]. In particular, this latter approach is mostly based on the potential use of metal complexes having N^6-substituted adenine ligands with therapeutic purposes. Nevertheless, future works are still needed to fully understand, at molecular level, the biochemistry of these molecules.

According to the aforementioned panorama, we have synthesized and structurally characterized novel ternary Cu(II) complexes with iminodiacetate-like chelators and different N^6-substituted adenines (Scheme 1). The aim of this work is to rationalize the molecular recognition patterns between such N^6-substituted adenines and copper(II) chelates where the tridentate chelator used (1) is unable to block the four closest coordination sites of the metal ion and (2) offers O-coordinated atoms as H-acceptor in intra-molecular interligand interactions. Note that the substituents of both chelating and N^6-R-adenine ligands are closely related (see Scheme 1). The novel compounds have been also investigated by spectral and thermal methods. Moreover, as the ligand 6-benzyladenine is a natural cytokinin. We compare, in the present paper, its activity with two related N^6-cycloalkyladenine derivatives, as well as the effect of Cu(II) coordination using the *Amaranthus* bioassay.

2. Experimental

2.1. Materials

Bluish $Cu_2CO_3(OH)_2$ was purchased from Probus. N-Methyliminodiacetic acid (H_2MIDA), 6-(dimethylamino)purine (HdimAP), 6-benzyladenine (HBAP), 6-(furfuryl)adenine (kinetine, Hkin) and thymine (Hthy) were supplied by Sigma-Aldrich. All reagents were used as received. N-benzyl- and N-(p-methylbenzyl)iminodiacetic acids (H_2NBzIDA and H_2MEBIDA, respectively) were synthesized in the acid form as reported in ref. [7]. N-Furfuryl-iminodiacetic acid (H_2FurIDA) was synthesized in the acid form according to an adapted procedure derived from that reported by Irving and da Silva et al. [22] and the aforementioned synthesis [7]. It should be noted that the pure ligand in its acid form (H_2FurIDA) is rather difficult to isolate whereas the monopotassium salt (KHFurIDA) crystallizes easily at neutral pH from the mother liquors of the synthesis. Further purifications can be performed by re-crystallization. Likewise, pure white samples of free H_2FurIDA acid can be obtained, at the expense of lower yields, by passing a concentrated aqueous solution of the monopotassium salt through an ion exchange column (by concentration under reduced pressure of the aqueous eluates with pH<4 and slow evaporation of the resulting aqueous solution). N^6-cyclohexyladenine (HCy6ade) and N^6-cyclopentyladenine (HCy5ade) were synthesised *de novo* by F. M. Albertí Aguiló et al. [23].

2.2. Syntheses of novel metal complexes

2.2.1. Synthesis of [Cu(NBzIDA)(HCy5ade) (H_2O)]·H_2O (**1**)

A blue solution of N-benzyliminodiacetate copper(II) chelate was prepared by reaction of $Cu_2CO_3(OH)_2$ (0.03 mmol, 0.006 g) and H_2NBzIDA acid (0.06 mmol, 0.013 g) in 10 mL of water, heating (50 °C) and stirring under moderate vacuum. Once the reaction of the binary chelate was completed, the solution was cooled down at room temperature. Then, an aqueous solution (10 mL) of the complementary base pair HCy5ade/Hthy (0.06 mmol, 0.012 g/0.008 g, respectively) was added over the binary chelate solution and let reacts. After 1 h, the reacting mixture was filtered on a crystallizing dish. Evaporation of the solvent was controlled with the aid of a plastic film. In three weeks, blue needle-like crystals suitable for X-ray diffraction (XRD) purposes appeared. One month later, colourless crystals were collected and identified as free thymine (Hthy) by FT-IR spectroscopy. Yield of this synthesis is ca. 85%. Elemental analysis (%): Calc. for $C_{21}H_{28}CuN_6O_6$ (**1**): C 48.08, H 5.29, N 16.18; Found: C 48.13, H 5.39, N 16.04. FT-IR (KBr, cm^{-1}) $\nu_{as}(H_2O)$ 3418, $\nu_s(H_2O)$ 3220, $\nu(N^6-H)$ 3235, $\nu(N-H)$ 3119, $\nu_{as}(CH_2)$ 2947, $\nu_s(CH_2)$ 2850, $\delta(H_2O)$ 1629, $\nu_{as}(COO)$ 1598, $\delta(N^6-H)$ 1539, $\delta(N-H)$ 1498, $\nu_s(COO)$ 1384, $\pi(C-H)_{ar}$ 709. The UV/visible spectrum shows an asymmetric d–d band with λ_{max} at 682 nm (ν_{max} 14,663 cm^{-1}).

2.2.2. Synthesis of [Cu(NBzIDA)(HCy6ade) (H_2O)]·H_2O (**2**)

A synthetic procedure similar to that of compound **1** was followed, using $Cu_2CO_3(OH)_2$ (0.06 mmol, 0.013 g), H_2NBzIDA acid (0.125 mmol, 0.028 g) and the complementary base pair HCy6ade/Hthy (0.125 mmol, 0.027 g/0.016 g, respectively) in 30 mL of water. After 1 h stirring, a micro-suspension was still observed within the reacting mixture what was indicative of the incomplete reaction of the adenine-like ligand. At the expense of lower yields, we decided to filter the solution. The crystallizing dish was allowed to stand at room temperature covered with a plastic film to control the evaporation of the solvent. Five days later, blue needle-like crystals suitable for XRD purposes were collected. After three weeks, colourless crystals appeared which were identified as free Hthy by FT-IR spectroscopy. Yield is ca. 65–70%. Elemental analysis (%): Calc. for $C_{22}H_{30}CuN_6O_6$ (**2**): C 49.15, H 5.33, N 15.49; Found: C 49.11, H 5.62, N 15.62. FT-IR (KBr, cm^{-1}) $\nu_{as}(H_2O)$ 3426, $\nu_s(H_2O)$ 3233, $\nu(N^6-H)$ 3227, $\nu(N-H)$ 3123, $\nu_{as}(CH_2)$ 2941, $\nu_s(CH_2)$ 2855, $\delta(H_2O)$ 1637, $\nu_{as}(COO)$ 1606, $\delta(N^6-H)$ 1541, $\delta(N-H)$ 1496, $\nu_s(COO)$ 1384, $\pi(C-H)_{ar}$ 707. The UV/visible spectrum shows an asymmetric d–d band with λ_{max} at 677 nm (ν_{max} 14,771 cm^{-1}).

2.2.3. Synthesis of [Cu(FurIDA)(HCy6ade) (H_2O)]·H_2O (**3**)

A blue solution of N-furfuryl-iminodiacetate copper(II) chelate was prepared by reaction of $Cu_2CO_3(OH)_2$ (0.06 mmol, 0.013 g) and H_2FurIDA acid (0.125 mmol, 0.026 g) in 15 mL of water, heating (50 °C) and stirring under moderate vacuum. In this case, HCy6ade

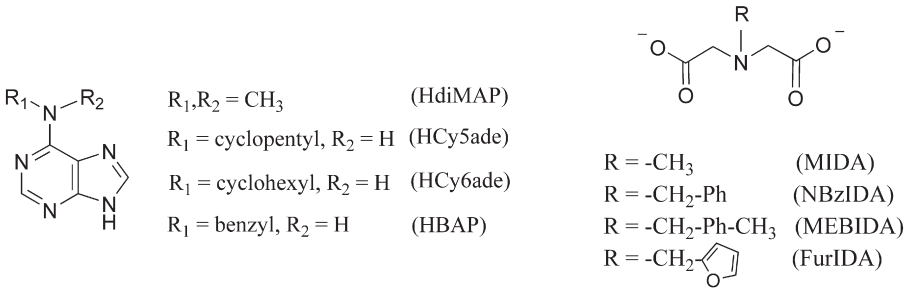

Scheme 1. Formulas of the N^6-substituted adenines and chelating ligands used in this work.

was directly added to the mother blue solution of the binary chelate (0.125 mmol, 0.027 g). However, a micro-suspension stood again after one hour of stirring and heating (25 °C). Then, the solution was filtered on a crystallizing dish at the expense of lower yields. The evaporation of the solvent was controlled with the aid of a plastic film. In ten days, blue parallelepiped crystals were collected for XRD studies. Yield of this synthesis is ca. 55–65%. Elemental analysis (%): Calc. for $C_{20}H_{28}CuN_6O_7$ (**3**): C 45.38, H 5.22, N 16.06; Found: C 45.50, H 5.34, N 15.92. FT-IR (KBr, cm^{-1}) $\nu_{as}(H_2O)$ 3415, $\nu_s(H_2O)$ 3285, $\nu(N^6-H)$ 3229, $\nu(N-H)$ 3123, $\nu_{as}(CH_2)$ 2936, $\nu_s(CH_2)$ 2856, $\delta(H_2O)$ and $\nu_{as}(COO)$ overlapped 1637, $\delta(N^6-H)$ 1541, $\delta(N-H)$ 1497, $\nu_s(COO)$ 1384, $\pi(C-H)_{ar}$ 640. The UV/visible spectrum shows an asymmetric d–d band with λ_{max} at 683 nm (ν_{max} 14,641 cm^{-1}).

*2.2.4. Synthesis of [Cu(MEBIDA)(HBAP) (H_2O)] · H_2O (**4**)*

A synthetic procedure similar to that of compound **3** was followed, using $Cu_2CO_3(OH)_2$ (0.25 mmol, 0.055 g), H_2MEBIDA acid (0.5 mmol, 0.118 g) and HBAP (0.5 mmol, 0.113 g) in 90 mL of water. The ligand HBAP did not seem to be soluble in the binary chelate liquors, then 20 mL of isopropanol were added. After 1 h stirring, the reaction was completed and the solution was filtered on a crystallizing dish covered by a plastic film. The solution dried off yielding only an amorphous blue product. Such residue was dissolved in 25 mL of acetonitrile and again covered with a plastic to control evaporation. One month later, blue prismatic crystals were collected, suitable for XRD purposes. Yield ca. 75%. Elemental analysis (%): Calc. for $C_{24}H_{28}CuN_6O_6$ (**4**): C 51.57, H 5.09, N 14.92; Found: C 51.47, H 5.04, N 15.01. FT-IR (KBr, cm^{-1}) $\nu_{as}(H_2O)$ 3423, $\nu_s(H_2O)$ 3266, $\nu(N^6-H)$ 3212, $\nu(N-H)$ 3150, two types of $\nu_{as}(CH_2)$ 2940 and 2923, $\nu_s(CH_2)$ 2857, $\delta(H_2O)$ 1635, $\nu_{as}(COO)$ 1611, $\delta(N^6-H)$ 1545, $\delta(N-H)$ 1496, $\nu_s(COO)$ 1391, $\pi(C-H)_{ar}$(HBAP) 705 and 644, $\pi(C-H)_{ar}$(MEBIDA) 752. The UV/visible spectrum shows an asymmetric d–d band with λ_{max} at 678 nm (ν_{max} 14749 cm^{-1}).

*2.2.5. Synthesis of [Cu(FurIDA)(HBAP)]$_n$ (**5**)*

A synthetic procedure similar to that of compound **3** was followed, using $Cu_2CO_3(OH)_2$ (0.25 mmol, 0.055 g), H_2FurIDA acid (0.5 mmol, 0.111 g) and HBAP (0.5 mmol, 0.113 g) in 100 mL of a 1:1 water: methanol mixture. After half an hour stirring and soft heating (25 °C), the reaction was completed and the solution was filtered on a crystallizing dish, covered by a plastic film to control the evaporation of the solvents. One month later, blue needle-like crystals were collected suitable for XRD purposes. Yield of this synthesis is ca. 70%. Elemental analysis (%): Calc. for $C_{21}H_{19}CuN_6O_5$ (**5**): C 50.51, H 3.80, N 16.93; Found: C 50.55, H 3.84, N 16.85. FT-IR (KBr, cm^{-1}) $\nu_{as}(H_2O)$ 3433, $\nu_s(H_2O)$ 3265, $\nu(N^6-H)$ 3206, $\nu(N-H)$ 3150, $\nu_{as}(CH_2)$ 2924, $\nu_s(CH_2)$ 2855, $\delta(H_2O)$ 1637, $\nu_{as}(COO)$ 1616, $\delta(N^6-H)$ 1546, $\delta(N-H)$ 1497, two types of $\nu_s(COO)$ 1382 and 1374, $\pi(C-H)_{ar}$ (HBAP) 703 and 644, $\pi(C-H)_{ar}$ (FurIDA) 598. The UV/visible spectrum shows an asymmetric d–d band with λ_{max} at 683 nm (ν_{max} 14,641 cm^{-1}).

*2.2.6. Synthesis of {[Cu(NBzIDA)(HdimAP)] · H_2O}$_n$ (**6**)*

A synthetic procedure similar to that of compound **3** was followed, using $Cu_2CO_3(OH)_2$ (0.25 mmol, 0.055 g), H_2NBzIDA acid (0.5 mmol, 0.116 g) and HdimAP (0.5 mmol, 0.082 g) in 80 mL of water. The reaction progressed rapidly without problems and the resulting solution was filtered on a crystallizing dish and left evaporates at r.t. controlled by the aid of a plastic film. Approximately two months later, blue crystals appeared. Nonetheless, such crystals were not suitable for XRD. Further re-crystallizations in isopropanol were carried out. After five months, well-shaped crystals appeared, suitable for XRD purposes. Yield of this synthesis is ca. 25%. Elemental analysis (%): Calc. for $C_{18}H_{22}CuN_6O_5$ (**6**): C 46.33, H 4.92, N 18.21; Found: C 46.40, H 4.76, N 18.04. $\nu_{as}(H_2O)$ 3433, $\nu_s(H_2O)$ 3251, $\nu(N-H)$ 3161, two types of $\nu_{as}(CH_3)$ 2978 and 2960, $\nu_{as}(CH_2)$ 2930, $\nu_d(CH_3)$ 2870, $\nu_s(CH_2)$ 2855, $\delta(H_2O)$ 1613, $\nu_{as}(COO)$ 1594, $\delta(N-H)$ 1492, $\delta(CH_2)$ 1451, $\delta_{as}(CH_3)$ 1443, $\delta_s(CH_3)$ 1430, $\nu_s(COO)$ 1384, $\pi(C-H)_{ar}$ (NBzIDA) 755, $\pi(C-H)_{ar}$ (HdimAP) 711. The UV/visible spectrum shows an asymmetric d-d band with λ_{max} at 688 nm (ν_{max} 14,535 cm^{-1}).

2.2.7. Synthesis of a related Cu(II) compound with N^6-furfuryl-adenine

A synthetic procedure similar to that of compound **3** was followed, using $Cu_2CO_3(OH)_2$ (0.25 mmol, 0.055 g), H_2NBzIDA acid (0.5 mmol, 0.116 g) and Hkin (0.5 mmol, 0.107 g) in 80 mL of water. The ligand Hkin did not seem to be soluble in the binary chelate liquors, then 20 mL of isopropanol were added dropwise until a clear blue solution was obtained. After 1 h stirring, the solution was filtered on a crystallizing dish and covered by a plastic film. After two weeks, very thin needle-like crystals were collected although they were not valid for XRD purposes. Crystallization on gel medium was performed to improve the size and the quality of the crystals, as described herein: H7deaA (0.02 mmol, 0.0027 g) was added as a solid powder to a vial. Afterwards, 2 mL of an 0.5% agar solution of Cu(NBzIDA) 0.01 M was added to the same vial, stirring the solution in a water bath (gentle heating) until the reaction took place. Then, the solution, properly capped, was left gel at room temperature. The vial stood at room temperature where larger crystals appeared within four weeks. However, neither these latter crystals provide good quality XRD data.

2.3. Crystallography

Measured crystals were prepared under inert conditions immersed in perfluoropolyether as protecting oil for manipulation. Suitable crystals were mounted on MiTeGen Micromounts™ and these samples were used for data collection. Data were collected with Bruker SMART APEX (**2** and **3**, 293 K), Bruker X8 KappaAPEXII (**4** and **5**, 100 K) diffractometers, whereas those of **1** and **6** were collected at the ESRF SYNCHROTRON BM16 beamline (Grenoble, France). The data were processed with APEX2 (**2**–**5**) [24] and HKL2000 (**1**, **6**) [25] programs and corrected for absorption using SADABS [26]. The structures were solved by direct methods [27], which revealed the position of all non-hydrogen atoms. These atoms were refined on F^2 by a full-matrix least-squares procedure using anisotropic displacement parameters [27]. All hydrogen atoms were located in difference Fourier maps and included as fixed contributions riding on attached atoms with isotropic thermal displacement parameters 1.2 times those of the respective atom. Geometric calculations were carried out with PLATON [28] and drawings were produced with PLATON [28] and MERCURY [29]. Additional crystal data and more information about the X-ray structural analyses are shown in Supplementary material S1 to S7. Crystallographic data for the structural analysis have been deposited with the Cambridge Crystallographic Data Centre, CCDC Nos. 906728–906733 from 1 to 6, respectively. Copies of this information may be obtained free of charge on application to CCDC, 12 Union Road, Cambridge CB2 1EZ, UK (fax: 44 1223 336 033; e-mail: deposit@ccdc.cam.ac.uk or http://www.ccdc.cam.ac.uk).

2.4. Amaranthus betacyanin bioassay

This bioassay was performed according to Biddington et al. [30] with the following modifications: *Amaranthus caudatus L.* seeds were germinated in Petri dishes with distilled water, in the dark, at 28 °C. In 7 days, ten cotyledons were cut at the hypocotyls level under dim green light (in order to avoid activation of betacyanin) and placed in a new Petri dish filled with 5 mL of treatment solution. The mother treatment solutions (200 μM) were prepared by dissolving the corresponding compounds (**1**–**4**) in a total volume of 10 mL of 100 μM KCl + 0.4 g L^{-1} Tyr. Moreover, a mother solution of N^6-benzyladenine, N^6-cyclohexyladenine and N^6-cyclopentyladenine were also prepared in the same conditions to be used as internal reference. From the mother solutions, curves of dilutions were carried out leading to different treatment solutions at 200, 50, 12.5, 3.125, 0.78, 0.195, 0.048 and 0.012 μM, respectively.

Please cite this article as: A. Domínguez-Martín, et al., Structural insights on the molecular recognition patterns between N^6-substituted adenines and N-(aryl-methyl)iminodiacetate copper(II) chelates, J. Inorg. Biochem. (2013), http://dx.doi.org/10.1016/j.jinorgbio.2013.02.002

After incubation of HBAP and the studied compounds, at 28 °C for 20 h, the cotyledons were placed in an Eppendorf tube with 1 mL of distilled water. Betacyanin was extracted by three freeze–thaw cycles with liquid N_2 (−70 °C) and sonication during 10 min. After centrifugation at 10,000 *g*, the supernatant was recovered and the betacyanin content was calculated by the difference in optical densities at 542 and 620 nm [31]. This procedure was repeated three times in order to ensure reproducibility of the bioassays.

2.5. Physical measurements

Analytical data were obtained in a Fisons–Carlo Erba EA 1108 elemental micro-analyser. Infrared spectra were recorded by using KBr pellets on a Jasco FT-IR 6300 spectrometer. TG analysis (pyrolysis) of the studied compounds (295–800 °C) were carried out in air flow (100 mL/min) by a Shimadzu Thermobalance TGA–DTG–50H instrument, and a series of FT-IR spectra (20–30 per sample) of evolved gasses were recorded for the studied compounds using a coupled FT-IR Nicolet Magma 550 spectrometer. Electronic (diffuse reflectance) spectra were obtained in a Varian Cary-5E spectrophotometer.

3. Results and discussion

3.1. Syntheses of the novel mixed-ligand copper(II) complexes

The syntheses were generally carried out according to the procedure previously reported by our research group [8–32]. This consists of a two-step reaction. First, the metal chelate is obtained by stoichiometric reaction of the appropriate iminodiacetic acid and basic copper(II) carbonate, according to reaction (a). Note that any other chelating agent used needs to be in their acid form and strong enough to react with the basic carbonate. The aim of this reaction is yielding only CO_2 as main by-product, easily removable by stirring, heating and moderate vacuum, thus avoiding the presence of undesired by-products (i.e. alkaline inorganic salts) that could interfere in the crystallization process.

$$Cu_2CO_3(OH)_2 + 2H_2L \rightarrow [CuL]\downarrow + CO_2\uparrow + 3H_2O \quad (a)$$

$$[CuL] + Hade/Hade : Hthy \rightarrow Cu(L)(Purine)\cdot nH_2O/ + Hthy \quad (b)$$

Afterwards, the binary compound is cooled down and the corresponding purine-like ligand is added. The reaction occurs under soft heating (max. 35 °C) and stirring. The addition of the purine ligand can be single or, when appropriate, as the complementary base pair Hade:Hthy according to reaction (b). This kind of syntheses using base pairs within ternary complexes was first introduced by us [8]. Our observations suggest that the use of appropriate base pairs, instead of the purine-like base alone, yields to more efficient incorporation of such latter ligand since the solubility of the system, in aqueous media, is increased [32]. Note that neutral thymine cannot bind the borderline copper(II) ion via its N-atom. Once the reaction is completed, the solution is filtered without vacuum to remove un-reacted products and left evaporate at room temperature. Although we usually work at r.t., temperature is also a key factor in the crystallization process that needs to be regulated (M.P. Brandi-Blanco, D. Choquesillo-Lazarte, A. Matilla-Hernández, J.M. González-Pérez, A. Castiñeiras, J. Niclós-Gutiérrez, J. Inorg. Biochem. (2013) submitted). The crystallizing dish is normally covered with a plastic film in order to the evaporation of the solvents. Besides, it also minimizes possible fungi and/or environmental contamination (i.e. fibbers of paper).

If systems are hypersaturated, micro-crystallization is usually observed during the first weeks. This products need to be cleared out by successive filtrations without vacuum in order to improve the quality of the crystals. Nevertheless, provided you obtain crystalline materials, is better to start from supersaturated solutions rather than non-saturated ones. Different approaches can also be done to improve the quality of the crystals that goes from re-crystallization in solvents with different polarities to diffusion experiments with different anti-solvents. A more sophisticated way to control the growth of crystals is using semisolid crystallization media, i.e. gels [33]. Furthermore, this procedure is also efficient for performing the aforementioned diffusion experiments or even preventing ageing phenomena in crystals [34].

The above described crystallization methods can be used in similar systems with transition metal ions, related chelating ligands and derivatives and/or analogues of nucleobases. For instance, Oscar Castillo el al. [35] describes similar synthetic routes although they typically use other inorganic salts as source of metal ions in their synthesis instead of basic carbonates. Times of crystallization cannot be directly related to crystallization processes but are really dependent on the solubility of the systems.

3.2. Molecular and crystal structure of $[Cu(NBzIDA)(HCy5ade)(H_2O)]\cdot H_2O$ (**1**)

Compound **1** consists of a complex molecule and one solvent molecule. In the complex, the copper(II) atom exhibits a 4 + 1 coordination polyhedron where the four closest donor atoms correspond to the tridentate NBzIDA chelating ligand (N10, O11, O21) and the N3(purine-like) donor of HCy5ade. Thus, NBzIDA ligand adopts a mer-NO_2 conformation. The apical coordination site is occupied by one aqua ligand. HCy5ade shows its most stable tautomer H(N9) Cy5ade what allows the cooperation of the Cu-N3 bond with an intra-molecular interligand H-bond [N9–H···O21(coord. carboxy, 2.724(2) Å, 131.9°) — Fig. 1, left]. Note that, in the crystal, the cyclopentyl moiety is disordered over two positions with an occupancy factor of 0.61/0.39. In this complex, the Cu(II) coordination environment is close to an elongated square-based pyramid, with a negligible basal distortion according to the estimated value of the Addison parameter $\tau = 0.02$ [36].

In the crystal of **1**, the complex molecules build 1D chains along the b axis by H-bonding interactions that involve the apical aqua ligands [O1-H1B···O22(non-coord. carboxy, 2.731(2) Å, 170.3°) — Fig. 1, right]. Moreover, inter-molecular C–H···π interactions between two disordered positions of the cyclopentyl moiety and the imidazole ring of HCy5ade stabilize the 1D chains [C65A–H65A···Cg, 2.71 Å, C–H···Cg 163°; C62B-H62D···Cg, 2.91 Å, 134°]. In addition, C22–O22···Cg interactions, involving the six-membered ring of HCy5ade, are identified within the 1D chains (see Table S7.1.). The polymeric chains are cross-linked by inter-molecular H-bonding interactions that comprise the non-coordinated water molecule, as donor and acceptor, and the Hoogstein face (N6 and N7 atoms) of the HCy5ade ligand (see Table S1.3.) giving rise to 2D layers. Hydrophobic forces accomplish the 3D array.

3.3. Molecular and crystal structure of $[Cu(NBzIDA)(HCy6ade)(H_2O)]\cdot H_2O$ (**2**)

Compound **2** consists of a molecular complex and one non-coordinated water molecule. The copper(II) atom is penta-coordinated, type 4 + 1. The NBzIDA chelator acts as a tridenate ligand, occupying three of the four closest sites around the metal centre (N10, O11, O21), in a mer-NO_2 conformation. Moreover, the Cu(II) coordination is satisfied by the N3(purine-like) donor from HCy6ade (in basal position) and one apical aqua ligand (Fig. 2, left). In this compound, the Addison parameter ($\tau = 0.01$) reveals an almost regular square-based pyramidal coordination. Again, the Cu-N3 bond cooperates with an intra-molecular interligand H-bonding interaction N9–H···O21(coord. carboxy, 2.736(4) Å, 131.8°), thus showing the ligand its most stable tautomer H(N9). Note that the cyclohexyl moiety is disordered over two positions with an occupancy factor of 0.75/0.25.

Please cite this article as: A. Domínguez-Martín, et al., Structural insights on the molecular recognition patterns between N^6-substituted adenines and N-(aryl-methyl)iminodiacetate copper(II) chelates, J. Inorg. Biochem. (2013), http://dx.doi.org/10.1016/j.jinorgbio.2013.02.002

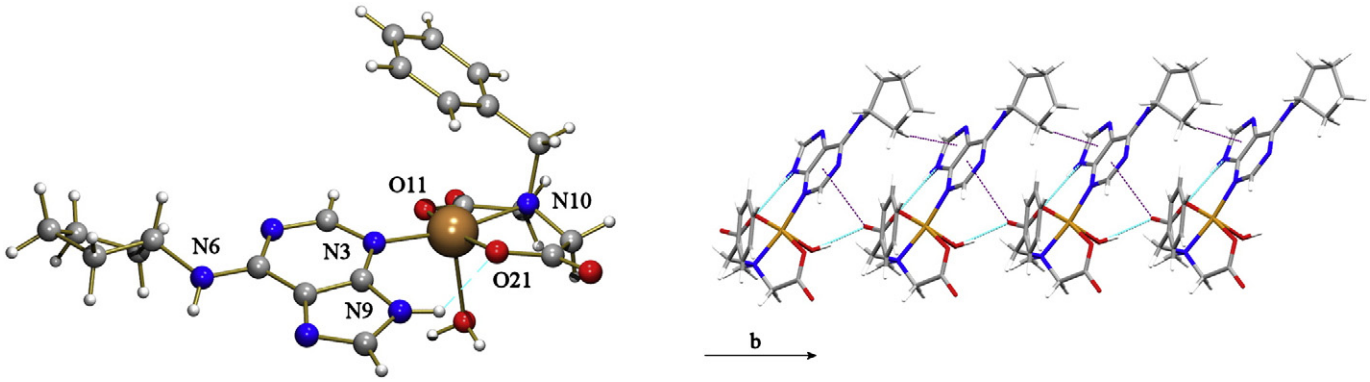

Fig. 1. Left: Molecular structure of [Cu(NBzIDA)(HCy5ade)(H_2O)] · H_2O (**1**). Only one of the two disordered positions for the cyclopentyl moiety is depicted for clarity. Bond distances (Å): Cu1 – O1 2.2966(11), Cu1 – N10 2.0058(12), Cu1 – O11 1.9381(11), Cu1 – O21 1.9683(10), and Cu1 – N3 1.9849(12). Right: View of the H-bonded 1D chain through the b axis highlighting the C – H · · · π and Y-X · · · π interactions in purple.

Compounds **1** and **2** display rather similar crystal packing (Fig. 2, right). The main difference between both crystals concerns the intra-chain C – H · · · π interaction that in **2** involves the cyclohexyl moiety of HCy6ade and the 5-membered ring of an adjacent HCy6ade ligand [C62A-H62A · · · Cg, 2.56 Å, 148°]. Besides this latter interaction, additional very weak intermolecular C – H · · · π interactions between the same cyclohexyl moiety and the 6-membered ring of HCy6ade ligand could also be considered (see Table S2.3. and Table S7.2.).

*3.4. Molecular and crystal structure of [Cu(FurIDA)(HCy6ade)(H_2O)] · H_2O (**3**)*

Compound **3** comprises one ternary complex molecule and one solvent molecule. Once more, the metal exhibits a slightly distorted square-based pyramidal coordination, type 4 + 1 (Addison parameter τ = 0.015), built by the N10, O11, and O21 donors of the tridentate FurIDA chelator (in mer-NO_2 conformation) and the N3 donor of the ligand HCy6ade.The apical position is occupied by one aqua ligand (Fig. 3). The apical position is occupied by an aqua ligand. Note that the furfuryl ring is disordered over two positions with an occupancy factor of 0.57/0.43. This molecular recognition pattern uses the most stable tautomer H(N9)Cy6ade, that can reinforce the Cu – N3 bond with an intra-molecular interligand H-bonding interaction N9-H · · · O21(coord. carboxylate, 2.742(4) Å, 130.7°).

Crystals of compounds **2** and **3** display nearly the same crystal packing. Indeed, N-benzyl and N-furfuryl pendant arms of the IDA chelating group play similar roles. This finding can be explained by the non-coordinating role of the O-heterocyclic atom, which is involved in the aromaticity of the furane ring, along with the similar steric hindrance caused by the furfuryl- and benzyl-substituents. In the crystal of **3**, two C – H · · · π interactions can also be considered (Fig. 4). The strongest interaction involves the cyclohexyl moiety of HCy6ade and the imidazole ring of an adjacent HCy6ade ligand [C62 – H62A · · · Cg, 2.61 Å, 140°]. The other is defined by the cyclohexyl moiety of HCy6ade and the pyrimidine ring of HCy6ade [C63 – H63B · · · Cg, 2.78 Å, 136°] (see Table S3.3. and Table S7.3.).

*3.5. Molecular and crystal structure of [Cu(MEBIDA)(HBAP)(H_2O)] · H_2O (**4**)*

The crystal of **4** also consists of a complex molecule and one non-coordinated water molecule. The copper(II) atom shows a 4 + 1 coordination polyhedron. The four closest Cu(II) donor atoms are supplied by the tridentate-chelating MEBIDA ligand (N10, O11 and O21), adopting a mer-NO_2 conformation, and the N3 donor of H(N9)BAP (Fig. 5, left). One aqua ligand occupies the apical site. Once again, the stability of the ternary complex is reinforced by the intra-molecular interligand interaction N9 – H · · · O21(coord. carboxy, 2.648(2) Å, 137.5°). Herein, the basal distortion of the coordination polyhedron is remarkably higher (τ = 0.20) than in the above-referred complex molecules **1**–**3**. This fact can be attributed to the implication of the N9-H group in a bifurcated H-bonding interaction, involving the latter referred intra-molecular interligand interaction and the N9 – H · · · O2(W, 2.962(2) Å, 128.7°) H-bond. Indeed, the dihedral angle between the plane of the purine moiety in HBAP and the mean basal coordination plane of the complex

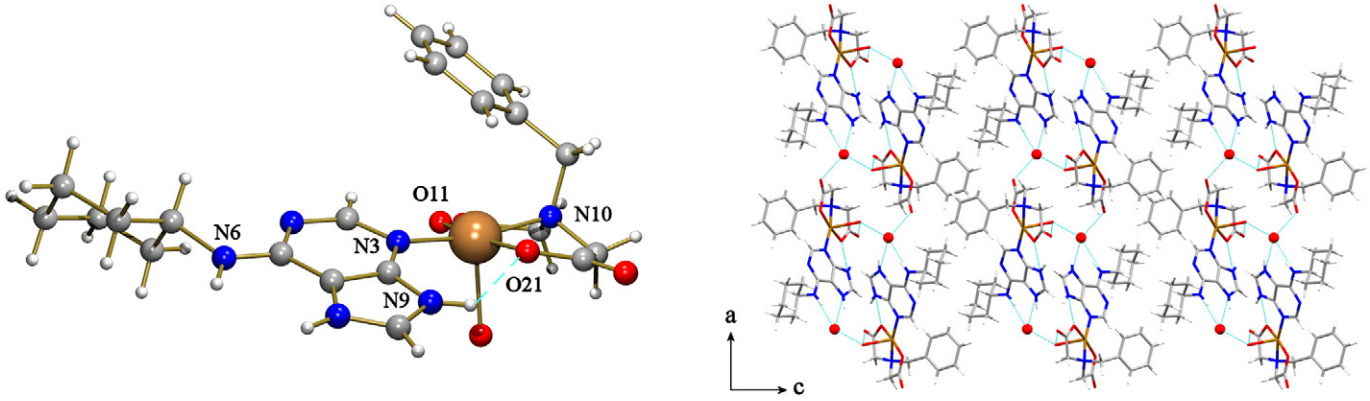

Fig. 2. Left: Molecular structure of [Cu(NBzIDA)(HCy6ade)(H_2O)] · H_2O (**2**). Only one of the two disordered positions for the cyclohexyl moiety is depicted for clarity. Bond distances (Å): Cu1 – O1 2.306(2), Cu1 – O11 1.935(2), Cu1 – O21 1.970(2), Cu1 – N10 2.003(3), and Cu1 – N3 1.988(3). Right: 3D network of compound **2** in the ac plane.

Please cite this article as: A. Domínguez-Martín, et al., Structural insights on the molecular recognition patterns between N^6-substituted adenines and N-(aryl-methyl)iminodiacetate copper(II) chelates, J. Inorg. Biochem. (2013), http://dx.doi.org/10.1016/j.jinorgbio.2013.02.002

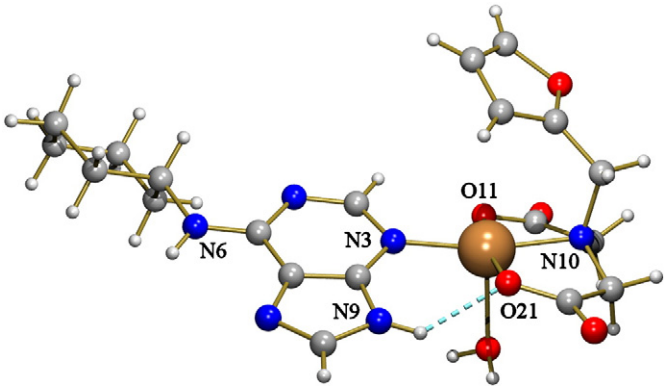

Fig. 3. Left: Molecular structure of [Cu(FurIDA)(HCy6ade)(H_2O)]·H_2O (**3**). Only one of the two disordered positions is depicted for the furfuryl arm for clarity reasons. Bond distances (Å): Cu1–O1 2.301(2), Cu1–O11 1.943(2), Cu1–O21 1.970(2), Cu1–N10 2.006(3), and Cu1–N3 1.978(3).

molecule in **4** (39.74°) is also higher compared to that of compounds **1**–**3** (~23°).

In the crystal of **4**, complex molecules build multi-stacked chains along the c axis by means of intermolecular π,π-stacking interactions between the 6-membered ring of the HCy6ade ligand and the aromatic moiety of the MEBIDA ligand appertaining to an adjacent molecule within the chain [Cg···Cg 3.541 Å, α = 6.56°, β = 9.75°, γ = 15.14° (Fig. 5, right)]. Besides, the aromatic moiety of MEBIDA ligand seems to involved in weak metal···π interactions within the complex molecules [Cu···Cg 3.753 Å, β = 43.21°]. Pairs of 1D chains are linked by symmetry related inter-molecular H-bonding interactions between the Hoogstein faces of two adjacent HBAP nucleobases [N6–H6···N7(HBAP, 2.981(2) Å, 164.0°)], building layers parallel to the ab plane that extra-stabilized by inter-molecular C–H···π interactions (see Table S7.4.). The 2D structure is further connected by H-bonds that involve the apical aqua ligand and solvent molecules giving rise to the 3D framework (see Table S4.3.).

3.6. Crystal structure of [Cu(FurIDA)(HBAP)]$_n$ (**5**)

The crystal of compound **5** is based on a coordination polymer built by the syn-anti bridging carboxylate group of FurIDA ligand. The metal exhibits a square-based pyramidal coordination, type 4 + 1. The N10, O11, and O21 donors of the tridentate mer-NO_2 FurIDA chelator and the N3 atom from HBAP satisfy the basal coordination plane. The apical position is occupied by the bridging O-atom from a carboxylate group of an adjacent FurIDA (Fig. 6, left). It is documented that the ligand N, N-bis(picolyl)furfurylamine (BPFur) acts as tripodal tetradentate chelator in [Cu(BPFur)Cl]ClO_4 [37] where the O-furfuryl donor weakly binds the metal centre [Cu–O 2.750(3) Å]. However, in compound **5** the O-furfuryl atom should not be considered as a donor atom for the copper(II) center since the corresponding Cu–O distance [Cu–O 2.951(3) Å] is according to a simple contact, close to the sum of Van der Waals radii are Cu (1.40 Å) and O (1.50 Å). The molecular recognition pattern between the Cu(FurIDA) chelate and the HBAP ligand is featured by the cooperative role of the Cu–N3 bond and the intra-molecular interligand N9-H···O21(coord. carboxy, 2.811(3) Å, 129.9°) H-bonding interaction. It is remarkably that the N9–H group also participates in an inter-molecular H-bond with nearly the same strength [N9–H···O11(coord. carboxy, 2.816(3) Å, 128.5°)]. This bifurcated interaction is the main responsible of the dihedral angle (32.86°) between the mean basal coordination plane and the purine moiety plane of HBAP. The trans-angles of the basal planes are quite similar so that the Addison parameter has a value close to τ = 0.01, as previously described for compounds **1**–**3**. Note that compounds **1**–**4** have similar molecular topology whereas compound **5** builds a polymer.

In the crystal of **5**, polymeric chains run along the c axis. Adjacent 1D chains are further associated by means of symmetry related H-bonds between the Hoogstein faces of two adjacent HBAP nucleobases [N6–H6···N7(HBAP, 3.000(3) Å, 156.4°)] building 2D layers where the ligands HBAP run along the 2_1 screw axes parallel to the bc plane (Fig. 6, right). Hydrophobic forces connect neighbouring layers to generate the 3D architecture. Despite both FurIDA and HBAP ligands have aromatic moieties, no stacking interactions have been observed in this compound.

3.7. Crystal structure of {[Cu(NBzIDA)(HdimAP)]·H_2O}$_n$ (**6**)

The crystal of compound **6** consists of polymeric chains that extend along the b axis and non-coordinated water. The copper(II) atom exhibits a nearly regular square-based pyramidal coordination (Addison parameter τ = 0.004), type 4 + 1, where the four closest donor atoms correspond to the tridentate NBzIDA chelating ligand (N10, O11, O21) and the N9(purine-like) donor of HdimAP. Thus, the NBzIDA ligand adopts a mer-NO_2 conformation. The apical donor is the O22 atom from the bridging carboxylate group of an adjacent NBzIDA ligand (Fig. 7, left). It is noteworthy that the dissociable proton in the HdimAP moiety is shifted to the N3 donor, showing the rare tautomer H(N3)dimAP. This tautomer allows to assist the bond Cu–N9 with an intra-molecular interligand H-bonding interaction N3–H···O11(coord. carboxy,

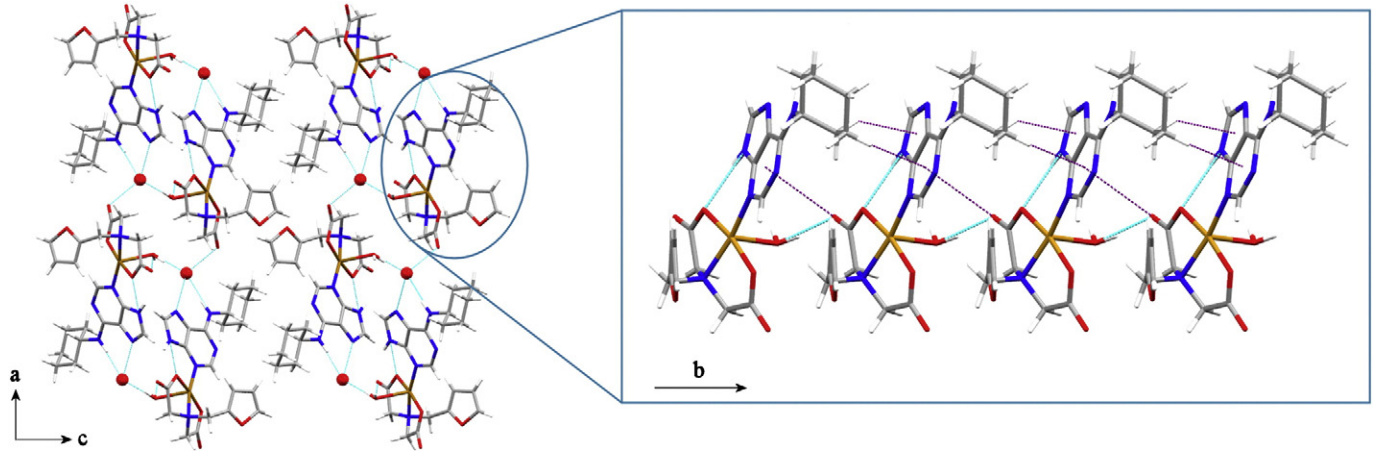

Fig. 4. View in the ac plane of the 3D architecture of [Cu(FurIDA)(HCy6ade)(H_2O)]·H_2O (**3**) with a detail of the 1D chain highlighting the C–H···π and Y–X···π interactions in purple.

Please cite this article as: A. Domínguez-Martín, et al., Structural insights on the molecular recognition patterns between N^6-substituted adenines and N-(aryl-methyl)iminodiacetate copper(II) chelates, J. Inorg. Biochem. (2013), http://dx.doi.org/10.1016/j.jinorgbio.2013.02.002

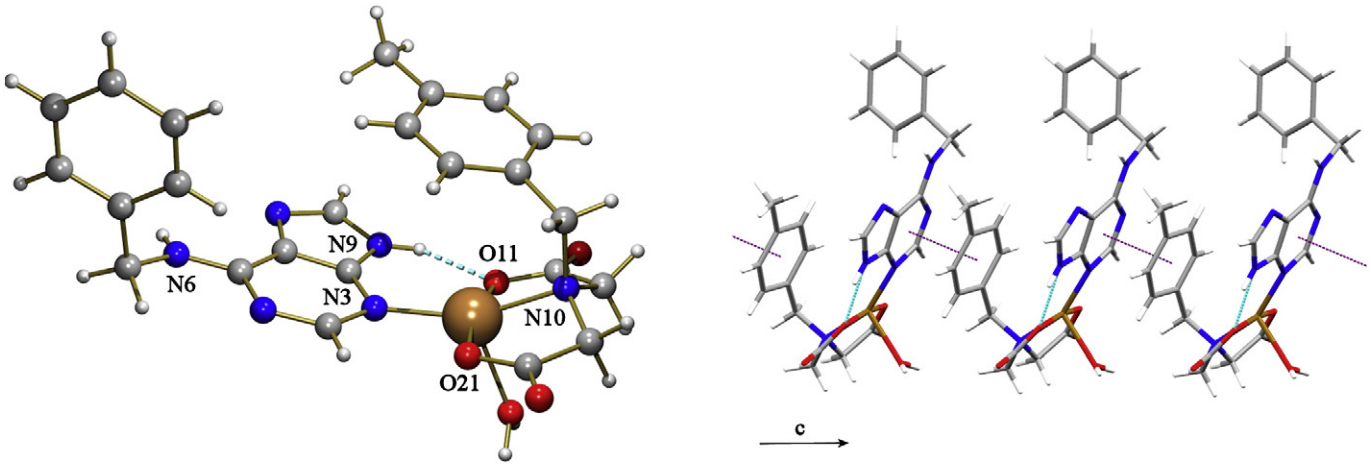

Fig. 5. Left: Molecular structure of [Cu(MEBIDA)(HBAP)(H_2O)]·H_2O (**4**). Bond distances (Å): Cu1 – O11 1.9485(14), Cu1 – O21 1.9524(14), Cu1 – N3 1.9963(17), Cu1 – N10 2.0203(17), and Cu1 – O1 2.2249(15). Right: Detail of multi-stacked 1D chains along the c axis.

2.728 Å, 133.9°). Note that this molecular recognition pattern is just the opposite of that referred for compounds **1**–**5**.

In the crystal of **6**, 1D polymeric chains extend throughout the b axis running along 2_1 screw axes. These latter chains connect each other building layers by means of H-bonding interactions that involve the solvent. In addition, the N3 – H group is also involved in a weak intermolecular H-bond [N3 – H · · · O1(W, 3.035(8) Å, 137.6°)] that help to stabilize the 2D structure (see Table S6.3.). Finally, hydrophobic interactions lead to the 3D architecture (Fig. 7, right). No stacking interactions are observed in this compound.

3.8. Metal binding of N^6-substituted adenines and future developments

The M – N3 + N9 – H · · · O metal binding pattern has been previously described by our research group and comprises metal complexes with Cu(II)-NBzIDA-like chelates and the nucleobase adenine [5,7,8]. Noticeably, the mononuclear complex [Cu(NBzIDA)(Hade)(H_2O)]·H_2O [7] shows the same formula and metal binding pattern that complexes **1**–**4** reported in this work. However, they are not isotype crystals since, therein, crystal packing was highly influenced by π,π-stacking interactions between the aromatic moieties of Hade and NBzIDA. Alternatively, the M – N3 + N9 – H · · · O recognition mode has also been observed in metal complexes with N^6-substituted adenine ligands such as HBAP [38] or HdimAP [39–41]. In particular, it should be remarked a very recent paper concerning the crystal structure of [Cu(μ_2-1,4-BDC)(HBAP)$_2$(H_2O)]$_n$ [40] (1,4-BDC = benzene-1,4-dicarboxylate(2-) anion), where each HBAP ligand recognizes the 1D-polymeric matrix Cu(μ_2-1,4-BDC)(H_2O) by means of the M-N3 bond plus the N9 – H · · · O(coord. carboxy) H-bonding interaction. Likewise, a search in the CSD restricted for neutral monodentate HdimAP ligand, with any metal ion, reveals only 4 hits [UFIDAP (Ru^{III}) [39], VABQOE (Re^{III}) [40], VABQUB (Re^{IV}) [40], VAZLOX (Rh^{I}) [41], in which HdimAP displays its most stable tautomer H(N9) and the molecular recognition consists of a coordination bond M – N3 + N9 – H · · · Cl

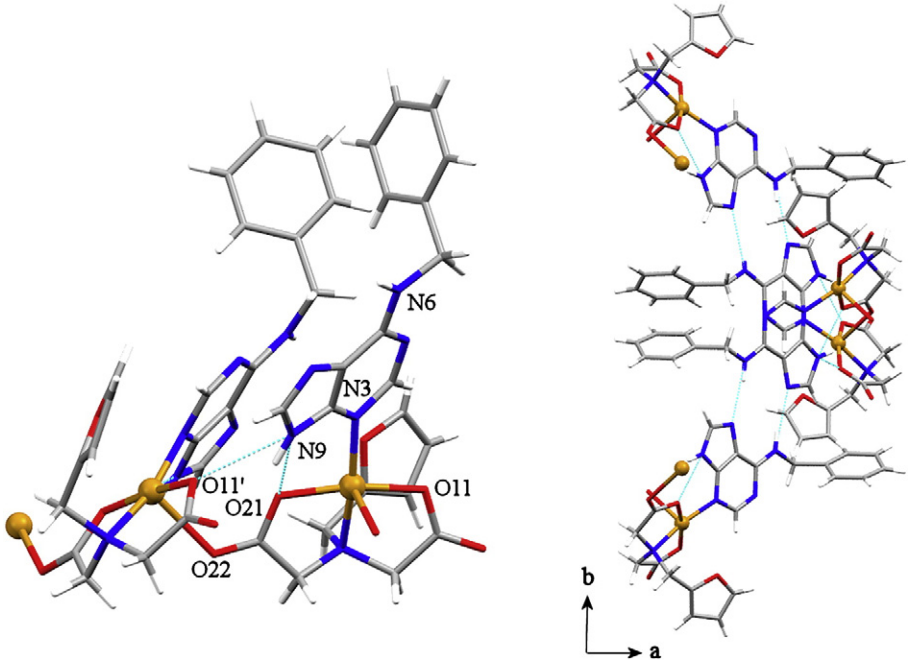

Fig. 6. Left: Molecular structure of [Cu(FurIDA)(HBAP)]$_n$ (**5**). Bond distances (Å): Cu1 – O21 1.930(2), Cu1 – O11 1.941(2), Cu1 – N3 1.987(2), Cu1 – N10 2.010(2), and Cu1 – O22(#1) 2.376(2); (#1 x,-y + 3/2,z-1/2). Right: View in the ba plane of one layer where adjacent chains connect by Hoogstein faces of HBAP ligands.

Please cite this article as: A. Domínguez-Martín, et al., Structural insights on the molecular recognition patterns between N^6-substituted adenines and N-(aryl-methyl)iminodiacetate copper(II) chelates, J. Inorg. Biochem. (2013), http://dx.doi.org/10.1016/j.jinorgbio.2013.02.002

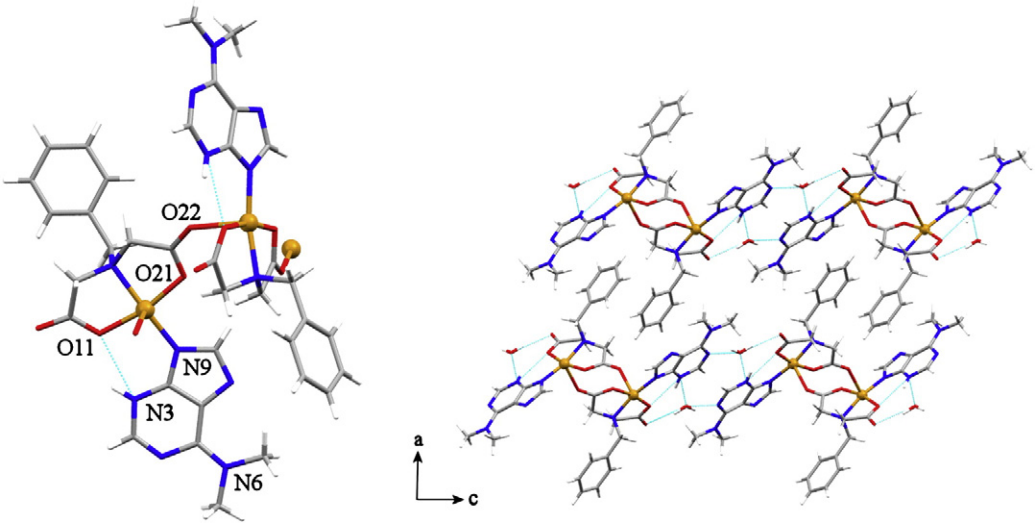

Fig. 7. Left: Molecular structure of $\{[Cu(NBzIDA)(HdimAP)]\cdot H_2O\}_n$ (**6**). Bond distances (Å): Cu1 – N10 2.007(5), Cu1 – O21 1.950(4), Cu1 – O11 1.953(4), Cu1 – N9 1.949(5), and Cu1 – O22(#1) 2.379(4); (#1 -x + 2,y-1/2,-z + 1/2). Right: 3D architecture in the ac plane of compound **6**.

intra-molecular interligand H-bond. This former pattern is similar to that showed previously in compounds **1**–**5** but also to those containing adenine [5]. Therefore, the recognition pattern N9 + N3 – H · · · O reported for compound **6** in this work is unprecedented for the HdimAP ligand. Nonetheless, the molecular reasons of this particular metal binding still remain quite unclear. In fact, a clear relationship could not be identified between the metal binding patterns displayed by HdimAP and the molecular/polymeric nature or the metal HSAB Pearson character of the reported compounds. Furthermore, the rare tautomer H(N3)purine-like has never been described for neutral purine-like ligands within mononuclear complexes. Indeed, it has been reported only twice regarding ternary binuclear compounds where adenine and 2,6-diaminopurine (Hdap) act as bridging ligands according to the formula: $[Cu_2(NBzIDA)_2(\mu_2\text{-N7,N9-H(N3)ade})(H_2O)_2]\cdot 3H_2O$ [8] and $[Zn_2(\mu_3\text{-benzene-1,4-dicarboxylate})(\mu_2\text{-N7,N9-H(N3)dap}]_n$ or $\{[Zn_2(\mu_4\text{-benzene-1,3,5-tricarboxylate})(\mu_2\text{-hydroxo})(\mu_2\text{-N7,N9-H(N3)dap}]\cdot H_2O\}_n$ [42].

In terms of nucleic acids, or their building blocks, the N3 donor (located in the minor groove of DNA) is generally disfavoured in comparison with the N7 donor, which is more accessible due to its location in the major groove of DNA. Moreover, N7 is more basic than N3 and this is consistent with their metal binding behaviour. According to B. Lippert and H. Sigel et al. [43], the alkylation of the exocyclic amino group has a relatively minor effect on the N-basicity order of the Hade (N9 > N1 > N7 > N3 ≫ N6). However, the presence of bulky substituents in the N^6-exocyclic amino group of purines hinders in a relevant way the N1 and N7 sites, driving the coordination through the minor groove binder N3. This metal binding behaviour is in accordance with the reported compounds **1**–**5** but also has previously been described for 9-methyl-dimAP. Although most of the interactions between metal ions and nucleic acids are described in the major groove, interactions within the minor groove of DNA should not be underestimated. Indeed, the minor groove is a relevant hydrogen acceptor group that could interact with enzymes, proteins or other active molecules and/or metal complexes. Thus, several promising minor groove binders have showed different biological activities such as antitumoral, antiprotozoal or antibacterial properties [44–47] and even other approaches regarding gene expression [48]. Therefore the interaction between different organic compounds and/or metal complexes with the N3(purine-like) donor is a topic of increasing interest and encourage further researches regarding the rational design of new biomimetic systems with biological and/or pharmaceutical applications.

3.9. Cytokinin activity

The Amanrathus betacyanin bioassay was highly homogeneous and reproducible for the cotyledon response to cytokinins. It has proved to be a very convenient method for testing series of compounds (see, for example ref. [49]). The cytokinin activity of HBAP, HCy5ade and HCy6ade ligands is shown in Fig. 8 (see Table S8). On the other hand, the *Amaranthus betacyanin* bioassay did not show any cytokinin activity for the tested Cu(II) complexes (**1**–**4**) in the studied range of concentrations. Effects of copper(II) overload were not observed in the plants what suggest that the compounds tested remains stable during the bioassay. Therefore, the lack of activity of Cu(II)-HBAP-like complexes could be understood considering the stability of the Cu-adenine bond which do not permit the correct interaction with cytokinin receptors. Thus, the absence of CK activity found in the metal complexes could be due to their inappropriate size, which would have limited their access to the protein active site, and/or because these complexes were not properly metabolized by the plant. To our knowledge, the N3, N9 moiety of the purine ring needs to be exposure in order to interact with the cytokinin receptors [50].

4. Concluding remarks

The molecular recognition patterns presented in this work highlight the role of N3 in those complexes containing N^6-monosubstituted adenine derivatives. Despite the N^6-ring substituent, aliphatic (**1**–**3**) or aromatic (**4**–**5**), and their molecular (**1**–**4**) or polymeric nature (**5**), in all the former compounds the Cu – N3 bond is reinforced by an intra-molecular interligand H-bonding interaction N9 – H · · · O. In contrast, in the polymer of compound **6**, the disubstituted ligand HdimAP exhibits the molecular recognition pattern Cu – N9 + N3 – H · · · O. Interestingly, this metal binding has not been reported before for this ligand or any neutral adenine-like ligand acting as monodentate. Since the N3(adenine) moiety is considered as a suitable target for metallo-drugs [51], further research needs to be carried out to better characterise the molecular details of DNA recognition by these molecules and/or metal complexes.

Acknowledgements

Financial support from Research Group FQM-283 (Junta de Andalucía) and MICINN-Spain (Project MAT2010-15594) is acknowledged. The project 'Factoría de Cristalización, CONSOLIDER INGENIO-2010' provided

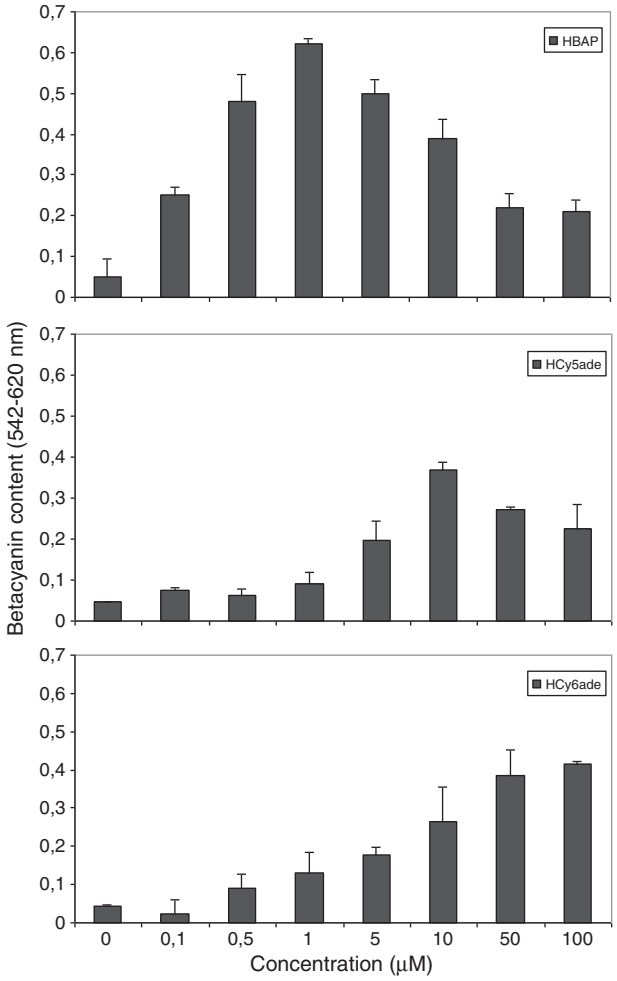

Fig. 8. Dose–response curves from 0.1 to 100 μM of HBAP, HCy5ade and HCyC6ade ligands in the Amaranthus betacyanin bioassay.

X-ray structural facilities for this work. Financial support from ERDF Funds and Junta de Andalucía to acquire the FT-IR spectrophotometer Jasco 6300 is acknowledged. ADM gratefully acknowledges ME-Spain for a FPU Ph.D Contract.

Appendix A. Supplementary data

Additional crystal data and structural information for 1–6 (S1-S6), analysis of π,π-stacking interactions and C–H···π (S7) and data about the *Amaranthus* bioassay (S8) are provided. For further information about the spectral properties (FT-IR and UV/visible) or Thermo-gravimetric analyses (TGA) carried out to all the reported compounds, please contact with the corresponding author. Supplementary data to this article can be found online at http://dx.doi.org/10.1016/j.jinorgbio.2013.02.002.

References

[1] B. Rosenberg, L. Van Camp, T. Krigas, Nature 205 (1965) 698–699.
[2] H. Sigel, Pure Appl. Chem. 76 (2004) 1869–1886.
[3] A. Terrón, J.J. Fiol, A. García-Raso, M. Barceló-Oliver, V. Moreno, Coord. Chem. Rev. 251 (2007) 1973–1986.
[4] B. Lippert, in: N.V. Hud (Ed.), Nucleic Acid – Metal Ion Interactions, RSC Publishing, 2009, (Chap. 2).
[5] D.K. Patel, A. Domínguez-Martín, M.P. Brandi-Blanco, D. Choquesillo-Lazarte, V.M. Nurchi, J. Niclós-Gutiérrez, Coord. Chem. Rev. 256 (2012) 193–211.
[6] A. Sigel, H. Sigel, R.K.O. Sigel, Interplay between Metal ions and Nucleic Acids — Metal Ions in Life Science, vol.10, Springer, the Netherlands, 2012.
[7] E. Bugella-Altamirano, D. Choquesillo-Lazarte, J.M. González-Pérez, M.J. Sánchez-Moreno, R. Marín-Sánchez, J.D. Martín-Ramos, B. Covelo, R. Carballo, A. Castiñeiras, J. Niclós-Gutiérrez, Inorg. Chim. Acta 339 (2002) 160–170.
[8] P.X. Rojas-González, A. Castiñeiras, J.M. González-Pérez, D. Choquesillo-Lazarte, J. Niclós-Gutiérrez, Inorg. Chem. 41 (2002) 6190–6192.
[9] T. Sorrell, L.A. Epps, T.J. Kistenmacher, L.G. Marcilli, J. Am. Chem. Soc. 99 (1977) 2173–2179.
[10] P. Amo-Ochoa, S.S. Alexandre, C. Pastor, F. Zamora, J. Inorg. Biochem. 99 (2005) 2226–2230.
[11] A.K. Mishra, R.K. Prajapati, S. Verma, Dalton Trans. 39 (2010) 10034–10037.
[12] L. Lua, C. Yi, X. Jian, G. Zheng, C. He, Nucleic Acids Res. 38 (2010) 4415–4425.
[13] C. Cao, K. Kwon, Y.L. Jiang, A.C. Drohat, J.T. Stivers, J. Biol. Chem. 278 (2003) 48012–48020.
[14] C.L. Price, M.R. Taylor, Acta Crystallogr. C52 (1996) 2736–2738.
[15] C.O. Miller, F. Shoog, M.H. Von Saltza, M. Strong, J. Am. Chem. Soc. 77 (1955) 1329–1334.
[16] H. Sakakibara, Annu. Rev. Plant Physiol. 57 (2006) 431–449.
[17] D.W.S. Mok, M.C. Mok, Annu. Rev. Plant Mol. Biol. 52 (2001) 89–118.
[18] S. Perilla, L. Moubayidin, S. Sabatini, Curr. Opin. Plant Biol. 13 (2010) 21–26.
[19] L. Szucova, Z. Travnicek, M. Zatloukal, I. Popa, Bioorg. Med. Chem. 14 (2006) 479–491.
[20] P. Starha, Z. Travnicek, I. Popa, J. Inorg. Biochem. 103 (2009) 978–988.
[21] J. Vicha, G. Demo, R. Marek, Inorg. Chem. 51 (2012) 1371–1379.
[22] H. Irving, J.J.R.F. da Silva, J. Chem. Soc. (1963) 1144–1148.
[23] Francisca M. Albertí Aguiló, Ph.D. Thesis; University of Palma de Mallorca, Spain, 2008.
[24] BRUKER, APEX2 Software, Bruker AXS Inc., Madison, Wisconsin, USA, 2010.(V2010.11).
[25] Z. Otwinowski, W. Minor, Methods Enzymol. 276 (1997) 307–326.
[26] G.M. Sheldrick, SADABS, Program for Empirical Absorption Correction of Area Detector Data, University of Göttingen, Germany, 2009.
[27] G.M. Sheldrick, Acta Crystallogr. A64 (2008) 112.
[28] A.L. Spek, PLATON. A Multipurpose Crystallographic Tool, Utrecht University, Utrecht, The Netherlands, 2010.
[29] C.F. Macrae, I.J. Bruno, J.A. Chisholm, P.R. Edgington, P. McCabe, E. Pidcock, L. Rodriguez-Monge, R. Taylor, J. van de Streek, P.A. Wood, J. Appl. Crystallogr. 41 (2008) 466.
[30] N.L. Biddington, T.H. Thomas, Planta 111 (1973) 183–186.
[31] C. Bigot, C. R. Acad. Sci. 266 (1958) 349.
[32] A. Domínguez-Martín, D. Choquesillo-Lazarte, J.M. González-Pérez, A. Castiñeiras, J. Niclós-Gutiérrez, J. Inorg. Biochem. 105 (2011) 1073–1080.
[33] J.M. García-Ruiz, M.L. Novella, R. Moreno, J.A. Gavira, J. Cryst. Growth 232 (2001) 165–172.
[34] A. Domínguez-Martín, D. Choquesillo-Lazarte, J.A. Dobado, I. Vidal, L. Lezama, J.M. González-Pérez, A. Castiñeiras, J. Niclós-Gutiérrez, Dalton Trans. (2013), http://dx.doi.org/10.1039/c2dt32191b.
[35] J.P. García-Terán, O. Castillo, A. Luque, U. García-Couceiro, P. Román, F. Lloret, Inorg. Chem. 43 (2004) 5761–5770.
[36] A.W. Addison, T.N. Rao, J. Reedijk, J. Van Rijn, G.C. Verschoor, J. Chem. Soc., Dalton Trans. (1984) 1349–1356.
[37] Y. Kani, S. Ohba, S. Ito, Y. Nishida, Acta Crystallogr. C56 (2000) e233.
[38] W.-B. Li, Acta Crystallogr. E67 (2011) m1249.
[39] B. Cebrian-Losantos, E. Reisner, C.R. Kowol, A. Roller, S. Schova, V.B. Arion, B.K. Keppler, Inorg. Chem. 47 (2008) 6513–6523.
[40] C. Pearson, A.L. Beauchamp, Inorg. Chem. 37 (1998) 1242–1248.
[41] W.S. Sheldrick, B. Gunther, J. Organomet. Chem. 375 (1989) 233–243.
[42] E.-C. Yang, Y.-N. Chan, H. Liu, Z.-C. Wang, X.-J. Zhao, Cryst. Growth Des. 9 (2009) 4933–4944.
[43] C. Meiser, B. Song, E. Freisinger, M. Peilert, H. Sigel, B. Lippert, Chem. Eur. J. 3 (1997) 388–398.
[44] P.G. Baraldi, A. Bovero, F. Fruttarolo, D. Preti, M.A. Tabrizi, M.G. Pavani, R. Romagnoli, Med. Res. Rev. 24 (2004) 475–528.
[45] R. Guddneppanavar, U. Bierbach, Anti-Cancer Agents Med. Chem. 7 (2007) 125–138.
[46] A. Klanicova, Z. Travnicek, J. Vanco, I. Popa, Z. Sindelar, Polyhedron 29 (2010) 2582–2589.
[47] A.I. Khalaf, C. Bourdin, D. Breen, G. Donoghue, F.J. Scott, C.J. Suckling, D. MacMillan, C. Clements, K. Fox, D.A.T. Sekibo, Eur. J. Med. Chem. 56 (2012) 39–47.
[48] A.V. Vargiu, A. Magistrato, Inorg. Chem. 51 (2012) 2046–2057.
[49] A. García-Raso, C. Cabot, J.J. Fiol, L. Spichal, J. Nisler, A. Tasada, J.M. Luna, F.M. Alberti, J.V. Sibole, J. Plant Physiol. 166 (2009) 1529–1536.
[50] J. Pas, M. von Grotthuss, L.S. Wyrwicz, L. Rychlewski, J. Barciszewski, FEBS Lett. 576 (2004) 287–290.
[51] R. Guddneppanavar, G. Saluta, G.L. Kucera, U.J. Bierbach, Med. Chem. 49 (2006) 3204–3214.